Journal of Applied Polymer Science

Effects of Micro and Nano β-TCP Fillers in Freeze-Gelled Chitosan Scaffolds for Bone Tissue Engineering

Nadeem Siddiqui, Krishna Pramanik
Department of Biotechnology and Medical Engineering, National Institute of Technology, Rourkela, Odisha 769008, India
Correspondence to: K. Pramanik (E-mail: kpr@nitrkl.ac.in)

ABSTRACT: Tissue engineering holds an exciting promise in providing a long-term cure to bone-related defects and diseases. However, one of the most important prerequisites for bone tissue engineering is an ideal platform that can aid tissue genesis by having biomimetic, mechanostable, and cytocompatible characteristics. Chitosan (CS) was chosen as the base polymer to incorporate filler, namely beta-tri calcium phosphate (β-TCP). This research deals with a comparative study on the properties of CS scaffolds prepared using micro- and nano-sized β-TCP as filler by freeze gelation method. The scaffolds were characterized for their morphology, porosity, swelling, structural, chemical, biodegradation, and bioresorption properties. Rheological behavior of polymer and polymer-ceramic composite suspensions were analyzed and all the suspensions with varying ratios of β-TCP showed non-Newtonian behavior with shear thinning property. Pore size, porosity of micro- and nano-sized composite scaffolds are measured as 48–158 μm and 77% and 43–155 μm and 81%, respectively. The scaffolds containing nano β-TCP possess higher compressive strength (∼2.67 MPa) and slower degradation rate as compared to composites prepared with micro-sized β-TCP (∼1.52 MPa). Bioresorbability, *in vitro* cell viability by 3-(4,5-dimethylthiazol-2-yl)-2,5-diphenyltetrazolium bromide (MTT) assay, proliferation by Alamar blue assay, cell interaction by scanning electron microscope, and florescence microscopy further validates the potentiality of freeze-gelled CS/β-TCP composite scaffolds for bone tissue engineering applications. © 2014 Wiley Periodicals, Inc. J. Appl. Polym. Sci. **2014**, *131*, 41025.

KEYWORDS: biodegradable; biomaterials; composites

Received 8 April 2014; accepted 13 May 2014
DOI: 10.1002/app.41025

INTRODUCTION

Osteo-chondral defects and diseases are one of the major concerns faced by patients round the globe and known to cause severe pain and finally loss of function. Scaffolds are three-dimensional (3D) temporary polymeric matrices which nest the cells by providing nourishment, direction, and thus facilitate the cells to develop into a new tissue. Bone is a nanostructured composite material which is arranged as an inorganic phase embedded into a predominant organic matrix.[1] The inorganic part is comprised of nanohydroxyapatite crystals that follow a discrete orientation within the organic matrix.[1–3]

Chitosan (CS), a linear polysaccharide obtained from deacetylation of chitin has been considerably used in tissue engineering applications due to its high biocompatibility, biodegradability, and intrinsic antibacterial property.[4] The most important characteristic of CS is, it can mold into different forms such as porous structures, gels, thin films, membranes, fibers which are favorable for cell growth.[5] The ability of CS to bind to growth factors makes it a competent candidate for scaffold material. Furthermore, the knack of linking CS to DNA can bring about a new hope in successful bone tissue engineering.[6]

Bone tissue engineering is mainly targeted at mimicking the nano architecture of natural bone.[7] It has been reported that natural or synthetic polymers alone may not be able to meet all the requirements of the budding bone cells.[8] Recent research, therefore, focuses on the development of artificial extracellular matrix by addition of bioceramics to suitable biopolymers. Bioceramics are light in weight, chemically stable, and compositionally similar to the mineral phase of the bone and, therefore, preferred as bone graft materials in hard tissue engineering.[9] In addition, these materials provide mechanical strength to the natural/synthetic biopolymers used for developing scaffolds.[10]

Beta tricalcium phosphate (β-TCP) belongs to the calcium phosphate ceramic group which falls under the category of bioactive ceramics. Its excellent biocompatibility, bone bonding, and bioresorption abilities single out β-TCP as a promising biofiller.[11] The osteointegrative property of β-TCP further makes it efficient to promote osteoblastic differentiation of stem cells.[12] Nano-sized materials were reported to offer better adsorption of selective proteins on the implant surface. The osteoblasts were found to attach more on nano-sized ceramic incorporated polymer-based composite scaffolds than microsized.[13]

Fabrication of 3D scaffold that can resemble natural extracellular matrix by a suitable technique is of paramount importance. In this context, freeze gelation is considered as a simple and economical method for fabrication of porous scaffolds.[14,15] This method can be used for producing scaffolds in less time with minimal energy requirement. In comparison with freeze drying, these scaffolds also posses negligible residual solvent which is favorable for cell culture, growth, and proliferation.[16]

Keeping in view of the above aspects, the present research work focuses on the development of CS-based composite scaffolds using β-TCP by freeze gelation method. There exists few reports on CS-based freeze-gelled scaffolds, using TCP, Wollastonite, and HAp as filler in micro dimension.[16–18] To the best of our knowledge, this is the first report on the usage of nano-sized β-TCP for developing CS/β-TCP freeze-gelled composite scaffold for bone tissue engineering. In this study, composite systems with varied ratios of micro- and nano-sized β-TCP fillers were prepared to investigate their impact on CS scaffold properties. Microstructural properties in terms of morphology, mechanical properties, and chemical properties have been investigated using these freeze-gelled scaffolds. Additionally, cytocompatability of these freeze-gelled scaffolds was evaluated to justify their role as effective biomaterials with enhanced bone tissue regeneration ability. The study has demonstrated the advantages of nano-sized β-TCP as filler for enhanced mechanical, decreased biodegradation rate, and increased biocompatibility over CS and micro-sized CS/β-TCP composite scaffolds.

EXPERIMENTAL

Materials

Chitosan, (CS- with a degree of deacetylation: $\geq$85) β-TCP powder in microsize [β-TCP (μ)] and nanosize [β-TCP (η)] were purchased from Sigma Aldrich Chemicals. Acetic acid, sodium hydroxide pellets, ethanol were procured from Merck (India) and used for scaffold development without any further purification. Dulbecco's Modified Eagle's medium (DMEM), Penicillin, Fetal bovine serum (FBS), Phosphate buffer saline (PBS) were purchased from Invitrogen and used for cell culture study. 5-dimethylthiazol-2-y1]-2, 5-diphenyl tetrazolium bromide (MTT), Calcien-AM fluorescent dye for cell viability assay, Alamar blue dye for proliferation assay and gluteraraldehyde for fixing the cells were procured from Sigma Aldrich Chemicals.

Preparation of CS Scaffold

CS was dissolved in aqueous acetic acid (0.1*M*) solution to form 2.5 wt % of CS polymer solution. The prepared CS polymer solution was poured in Petri dishes and kept at -20°C for 6 h. The Petri dishes containing frozen CS solution was immersed in a precooled gelation medium consisting of 70 : 30 (v/v) NaOH: EtOH.[19] The Petri dishes were kept at -20°C for 6 h until gelation occurs below the freezing point of CS solution. The Petri dishes were removed from gelation medium and vacuum dried (Daihan Labtech, Korea) for 6–8 h at 40°C. The scaffolds were finally rinsed thoroughly with PBS and deionized water thrice followed by drying. The scaffolds were cut into specific dimensions and made ready for different characterization techniques.

Preparation of CS/β-TCP Composite Scaffold

β-TCP powder (microsize and nanosize) was added individually to the prepared CS solutions in different weight ratios (CS: β-TCP) as 90 : 10, 80 : 20, 70 : 30, 60 : 40, and 50 : 50. To ensure a homogeneous solution, the mixture was stirred continuously overnight, with a magnetic stirrer at room temperature. Then, the above mentioned protocol (used for CS scaffold) was followed for preparing CS/β-TCP composite scaffold. The composite scaffolds were also cut into specific dimensions and used for further experiments.

CHARACTERIZATION

Morphological Analysis

The morphology of the prepared CS and CS/β-TCP composite scaffolds was analyzed by scanning electron microscope (SEM, JEOL-JSM 6480LV, Japan). The traces of moisture present in the scaffolds were completely removed by a vacuum drier for 2 h at 40°C. A platinum coater (Quorumtech, Q150RES, Czech Republic) was used for coating the scaffolds for 60 s. A minimum of 25 pores were considered for calculating the pore size of scaffolds using IMAGE J software.

Phase Analysis

The phase analysis of CS and CS/β-TCP composite scaffolds was performed by X-ray Diffractometer (PANalytical, X'pert Philips) using Cu-Kα radiation in a step-scan mode in the 2θ range of 10–80° with a scanning speed of 2° per minute at 30 kV and 30 mA.

Structural Analysis

Fourier transform infrared spectroscopy (FTIR) was performed to evaluate the structural property of the prepared CS and CS/β-TCP composite scaffolds using Infrared Microscope (Shimadzu AIM-8800, Japan). Hydraulic press was used to pelletize the samples by mixing with dry KBr powder.[20] The machine was operated in transmittance mode in a scanning range of 500–4000 cm^{-1} with a resolution of 8 cm^{-1}.

Rheological Behavior

The viscosity of the prepared CS solution and CS/β-TCP composite suspensions was analyzed by rotational cone (diameter = 30 mm; angle = 5.4°) and plate viscometer (Bohlin Visco-88, Malvern, UK). A constant gap of 0.15 mm was maintained between cone and the plate throughout the study. The variable shear rate applied was in the range of 20–100 s^{-1} for 16 min.[21] All the samples were analyzed at room temperature. Rheological data were analyzed and apparent viscosity was calculated using cross model (Bohlin visco-8 software).

Porosity Measurement

The porosity of CS and CS/β-TCP composite scaffolds was measured by mercury intrusion porosimeter (Poremaster-33, Quantachrome). The bulk density of the scaffolds was measured by liquid displacement method. The percentage porosity was calculated from intrusion data according to Washburn equation, $D=(1/P)4\gamma(\cos\varphi)$. The various parameters of the equation are: D is the pore diameter, γ is surface tension of mercury, φ is the contact angle between mercury and the pore wall, and P is the applied pressure.[22] All the experiments were performed in triplicates.

Swelling Study

Swelling study was performed on CS and CS/β-TCP composite scaffolds in deionized water at room temperature until they reach equilibrium, that is, reaching a constant wet weight. Excess water present on the scaffold surface was wiped out and dry weight was noted.[23] The percentage swelling was calculated by the following formula using Mathtype 5.0

$$\%\text{Swelling} = (\text{WET}_{wt} - \text{DRY}_{wt})/\text{DRY}_{wt} \times 100 \quad (1)$$

Mechanical Property

Compressive strength of developed CS and CS/β-TCP composite scaffolds was analyzed by Universal testing machine (H10KS, Tinius Olsen). The compression test on scaffolds (10-mm diameter × 8-mm thickness) was performed with a crosshead speed of 0.01 mm/s. Compression values were obtained from the initial slope of stress strain plot. Three parallel samples were evaluated for each kind of scaffold.[24]

In vitro Biodegradation Study

In vitro biodegradation of developed CS and CS/β-TCP composite scaffolds were performed in simulated body fluid (SBF) following the procedure described elsewhere.[6] The dry weight of the scaffold sample was weighed and designated as W_I. The sample was immersed in a beaker containing 15 mL of SBF, kept oscillating at 37.0 ± 0.5°C. After soaking for 1, 7, 14, 21, and 28 days, sample was withdrawn from SBF, gently rinsed with deionized water and weighed after freeze drying. The weight of the resulted sample is noted as W_F. The remaining weight percentage (W_R) was calculated according to the formula (using Mathtype 5.0) given below. All the experiments were performed in triplicates.

$$W_R = \frac{W_F}{W_I} \times 100 \quad (2)$$

Bioresorption Analysis

To evaluate the bioactivity of the composite scaffolds *in vitro*, 1 g of scaffold was immersed in 15 mL SBF and incubated at 37°C for 1, 7, 14, and 21 days following standard protocol.[25] After each time point, the scaffold was taken out, rinsed with distilled water, freeze dried, and finally observed for the morphology of crystals formed on the surface using a SEM (JEOL-JSM 6480LV, Japan).

Cell Culture and Cell Seeding

Mesenchymal stem cells (MSCs) were isolated from umbilical cord blood and cultured in an expansion medium consisting of 90% DMEM, 10% FBS, and 1% antibiotic solution.[26] Media was changed every alternate day and the cells were subcultured up to fourth passage. Scaffolds were sterilized prior to cell seeding by 70% ethanol treatment for 2 h, followed by PBS wash. The scaffolds were incubated in culture medium prior to cell seeding. Cells were seeded on the scaffolds with a pay load of 5×10^4 cells/mL by static method.

Metabolic Activity and Proliferation Assay

Cell seeded scaffolds were incubated at 37°C under 5% CO_2 for 3, 5, and 7 days. The metabolic activity of composite scaffolds was analyzed by MTT ([5-dimethylthiazol-2-y1]-2, 5-diphenyl tetrazolium bromide) assay following the procedure reported earlier.[27] Briefly, 10 μL of MTT solution (5 mg/mL) was added and to the cell suspension and culture plates were incubated at 37°C for 4 h. DMSO of 100 μL was used to solubilize formazan and absorbance was measured at 595 nm in a microplate reader (2030 multi label reader Victor X3, Perklin Elmer). Pure CS scaffold was used as control.

Proliferation of hMSCs on CS/β-TCP freeze-gelled composite scaffolds was examined by Alamar blue dye reduction assay at time intervals of 3, 5, and 7 days. The change in color is attributed to the reduction of dye by mitochondrial enzymes.[28] Hundred microliter of Alamar blue was added to the scaffolds in 1 mL of media and incubated for 5 h at 37°C. The absorbance was measured at 570 nm using a multiplate reader (2030 multi label reader Victor X3, Perklin Elmer). The proliferation rate was calculated according to the manufacturer's protocol.

Cell Attachment and Florescence Microscopy

Cell attachment on scaffolds was evaluated by observing morphology of the constructs with the help of SEM (JEOL-JSM 6480LV, Japan). Gluteraldehyde solution [2% (v/v)] was used for fixing the cultured cells. Samples were rinsed with wash buffer thrice and a series of ethanol wash was done and finally the samples were air dried.[22] The scaffold samples were stained with calcein-AM and incubated for 30 min.[29] PBS was used for washing of the stained samples and morphology of cell scaffold construct was observed under fluorescence (Carl Zeiss, Axiovert 40CFL) microscope.

Statistical Analysis

Most of the results were obtained from triplicate samples. A statistical difference was established for $P < 0.05$, $P < 0.02$, and student t test was used for statistical analysis.

RESULT AND DISCUSSION

Development of Scaffolds

Scaffolds were prepared by freeze gelation method which is economical, takes less time, and minimal energy.[14] Sodium hydroxide (NaOH) present in the gelation mixture aids in neutralizing the acidic effects of acetic acid and prevents the formation of surface skin.[19] The developed scaffolds were labeled as—pure CS scaffolds:-CS, composite scaffolds with β-TCP is in micro-size and nanosize were labelled as CTM and CTN, respectively. The composite scaffolds with varied micro- and nano-TCP weight ratios were CTM90 : 10, CTM80 : 20, CTM70 : 30, CTM60 : 40, and CTM50 : 50 and CTN90 : 10, CTN80 : 20, CTN70 : 30, CTN60 : 40, and CTN50 : 50, respectively.

Morphological Analysis

It has been reported that adequate pore size and interconnectivity of pores in scaffolds are vital factors for transport of oxygen and nutrients to the cells.[30] SEM images were used to visualize these features. Figure 1(a,b) illustrates excellent interconnected pores in pure CS scaffold with 61–171 μm pore size range. In case of scaffolds consisting of nano β-TCP, the pores are regular [Figure 1(e,f)] with a pore size range of 43–155 μm. Uniform distribution of nano TCP is observed on the pore walls of composite scaffolds as shown in Figure 1 (e,f). The pore size obtained with micro β-TCP is in the range of 54–158 μm. Furthermore, agglomeration (represented in arrow marks) of micro β-TCP is found to occur beyond a certain limit (weight ratio)

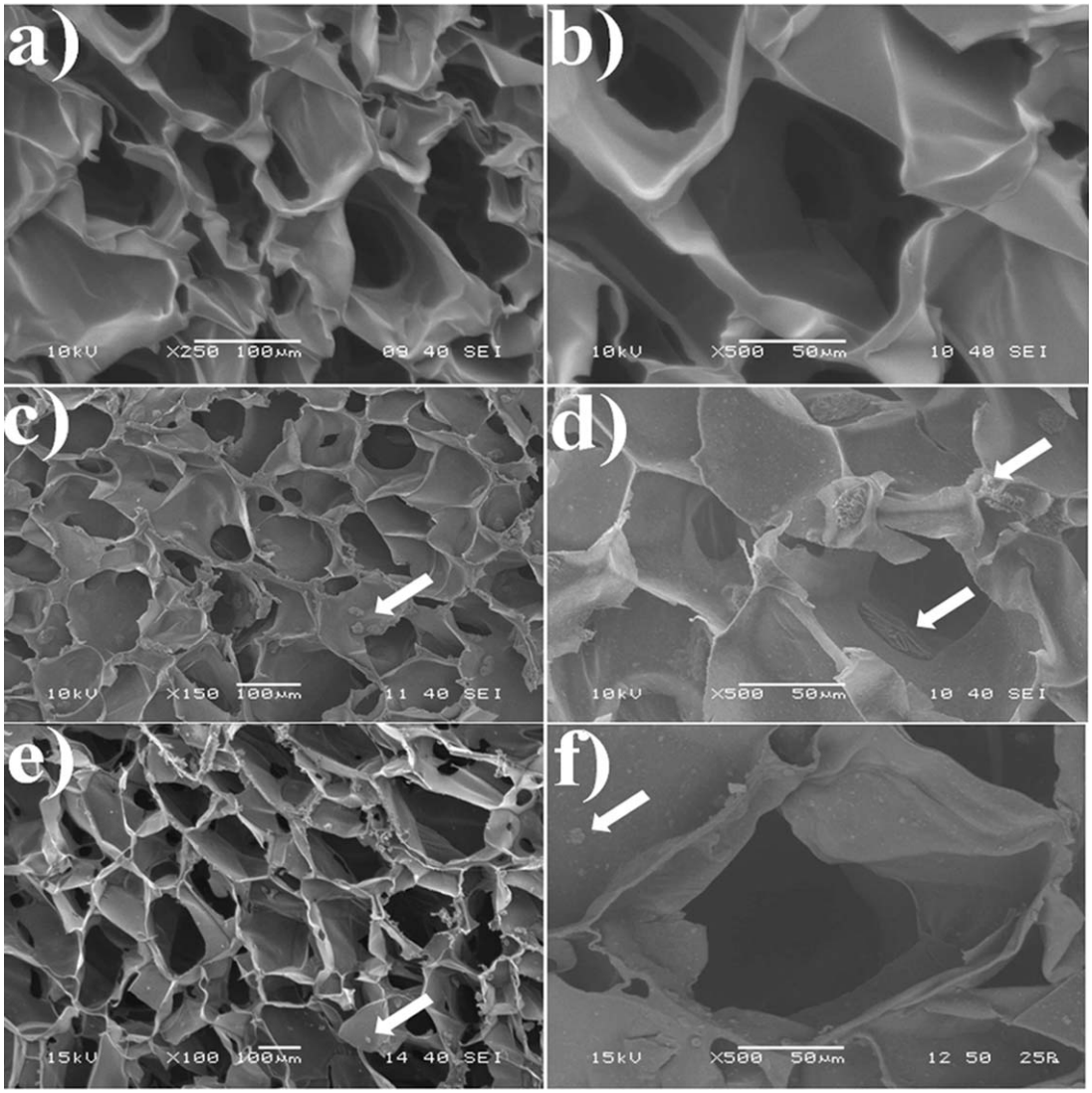

Figure 1. Morphology of pure CS (a, b) and CS/β-TCP composite [CTM 70 : 30 (c, d)], [CTN 80 : 20 (e), 70 : 30 (f)] freeze-gelled scaffolds. Agglomerates of β-TCP (c, d) are represented with white color arrow marks. Uniform distribution of nano β-TCP (e, f) on pore walls of scaffolds is shown with white color arrow marks.

as shown in Figure 1(c,d). The pore size range obtained with various ratios of micro and nano β-TCP is shown in Table I. Published reports suggest that the pore size of scaffolds should be in the range of 65–300 μm for bone tissue engineering applications and result obtained in our study matches with the reported pore size range.[31,32] Thus, the developed freeze-gelled CS and CS/β-TCP composite scaffolds had the required morphological necessity for the cell growth and proliferation of osteocytes.

Phase Analysis

Pure CS scaffold showed a dome shaped curve which indicates its amorphous nature whereas in composite scaffolds, the CS peak was completely dominated by incorporation of ceramic which is attributed to high crystalline nature of β-TCP. Pure CS showed a prominent peak at $2\theta = 20.8$, where as two prominent peaks of β-TCP were found at 31.5 which confirms the presence β-TCP in the composite.[8] Thus, it is established that the crystallinity of the composite scaffold is much higher than the pure CS scaffold due to addition of β-TCP which is shown in Figure 2(a).

Structural Analysis

An infrared spectrum represents a fingerprint of a material with absorption peaks. Thus, infrared spectroscopy can provide a positive identification of every different constituent present in the composite. IR analysis of CS and CS/β-TCP scaffolds was done to reveal the interactions between the individual components present and to confirm the presence of chemical constituents in the scaffold. The peaks generated as a result of chemical interactions is shown in Figure 2(b). Pure CS scaffold showed peaks around 897 and 1154 cm^{-1} of assigned saccharide structure and the characteristic peaks of N—H bending of CS was observed at 1560 cm^{-1}.[33] The peak range typical for tetrahedral anions is from 790 to 1190 cm^{-1}. Our analysis demonstrated PO_4^{-3} peaks at 1040, 1122, 610, and 551 cm^{-1} fall within the

Table I. Pore Size, Porosity, and Mechanical Strength of Chitosan and Chitosan/β-TCP Freeze-Gelled Scaffolds with Different Ratios

Scaffold type	Pore size (μm)	% Porosity	Compressive strength (MPa)
CS	61–171	87 ± 3.21	0.19 ± 0.05
CTM [90 : 10]	48–158	80 ± 2.33	0.51 ± 0.09
CTM [80 : 20]	54–154	79 ± 4.96	0.74 ± 0.06
CTM [70 : 30]	58–148	77 ± 3.21	1.52 ± 0.09
CTM [60 : 40]	64–143	75 ± 6.1	1.39 ± 0.05
CTN [90 : 10]	43–155	85 ± 2.65	1.76 ± 0.11
CTN [80 : 20]	45–149	81 ± 3.43	2.67 ± 0.13
CTN [70 : 30]	46–141	79 ± 2.87	2.49 ± 0.19
CTN [60 : 40]	49–136	73 ± 3.6	2.16 ± 0.21

Abbreviations: CS, chitosan; CTM, chitosan micro β-TCP scaffold; CTN, chitosan nano β-TCP scaffold.

reported range.[34] Reports suggest peak shifts and formation of new peaks due to interaction of ceramic with the polymer functional groups.[35] IR analysis proved a slight peak shift and formation of new peaks due to presence of β-TCP in composite scaffolds. The peaks ranging from 1560 to 1587 cm^{-1} N—H bending has been shifted to 1556–1573 cm^{-1} which may correspond to the interaction of β-TCP with CS. The peaks around 1000–1300 cm^{-1} were due to the interaction of phosphate with oxygen and nitrogen of pure CS. Furthermore, there is no difference is observed in the peaks of composite scaffolds with the varying amount of β-TCP as reported earlier.[36]

Rheological Behavior

The flow behavior of a polymer solution has been reported to depend on the composition and stability of the composite suspensions.[34] Viscosity was, therefore, analyzed for both polymer and polymer-ceramic suspensions under varied shear stress. All the solutions have shown non-Newtonian behavior with shear thinning property as illustrated in Figure 3.[21,37] CS solution has lower viscosity (1.21 Pas) in comparison to CS/β-TCP composite solutions (1.24–1.99 Pas). CS solution with micro β-TCP as filler has shown higher viscosity (1.31–1.42 Pas) when compared to nano TCP (1.24–1.36 Pas). It is further observed that as the concentration of bioceramic increased in polymer, viscosity has been gradually increased in a linear fashion as illustrated in Figure 4(b). The homogenity of composite solution is observed to decrease as TCP concentration increases. As a result, the layers in the composite suspension begun to show restricted movement cumulating in increased viscosity.[34,38] As such, there is no direct correlation between final scaffolds with non Newtonian behavior of CS solution and CS/β-TCP suspension, an alteration in viscosity of polymer ceramic composite suspension is found to have an impact on pore size of the developed scaffolds. The pore size of composite scaffolds is less than pure CS scaffold. This decrease in pore size is due to the reduced mobility of high viscous CS/β-TCP composite suspensions. The ice crystal mobility responsible for pore diameter

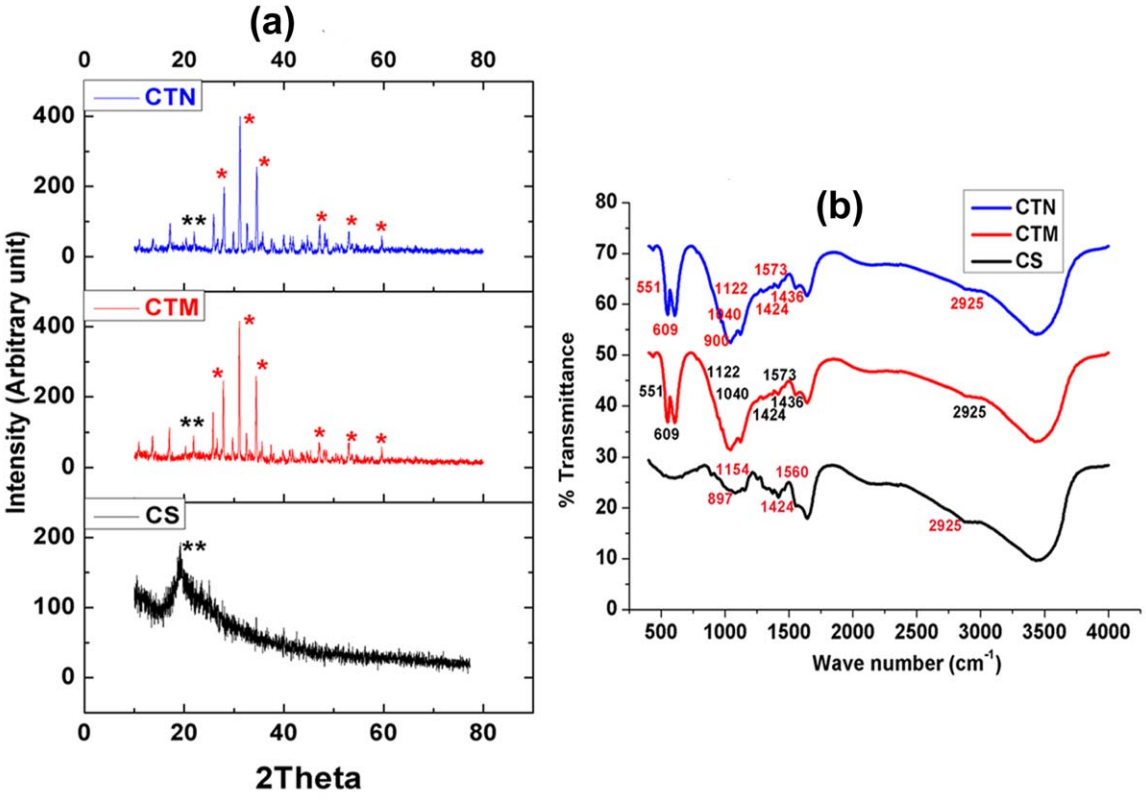

Figure 2. X-ray diffraction (XRD) (a) and Fourier transform infrared (FTIR) (b) patterns of CS and CS/β-TCP freeze-gelled scaffolds. [Color figure can be viewed in the online issue, which is available at wileyonlinelibrary.com.]

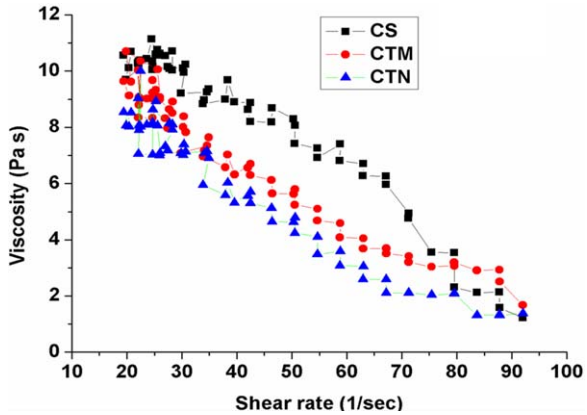

Figure 3. Rheological behavior of CS and CS/β-TCP blend solutions. [Color figure can be viewed in the online issue, which is available at wileyonlinelibrary.com.]

is reduced in high viscous suspensions[39] and hence a decrease in pore size of composite scaffold is observed when compared to pure CS scaffolds.

Porosity

The porosity of scaffold is an important parameter which decides not only the transport of materials necessary for cell nutrition, but also the cell attachment and migration.[40] Pure CS scaffold has shown a porosity of 87 ± 3.21%. A slight decrease in porosity is observed with composite scaffolds having micro β-TCP and nano β-TCP as 77–80% and 79–85%, respectively. The % porosity of all other samples with varied ratios of β-TCP were measured and depicted in Table I. Furthermore, nano β-TCP particles are observed to be homogenously distributed in the polymer matrix, where as micro-sized particles are found to agglomerate. The agglomeration was reported earlier with hydroxy apatite reinforcement.[10] Because of this unique distribution of β-TCP in the polymer matrix there exists a gradation in the % porosity. The trend observed is illustrated in Figure 4(a).

Swelling Study

The ability of the scaffolds to swell represents their hydrophilic nature. Swelling behavior of CS and CS/β-TCP composite scaffolds is presented in Figure 3(c). The scaffolds show a saturated swelling state during initial hours of soaking in deionized water without showing any disintegration or dissolution, thus preserving physical integrity. The scaffolds [Figure 4(c)] have shown a rapid swelling indicating their excellent hydrophilic nature.[35] Among the developed scaffolds, pure CS scaffold shows a higher swelling percentage (~326%) than that of CS/β-TCP composite scaffolds. Furthermore, the swelling property decreases with

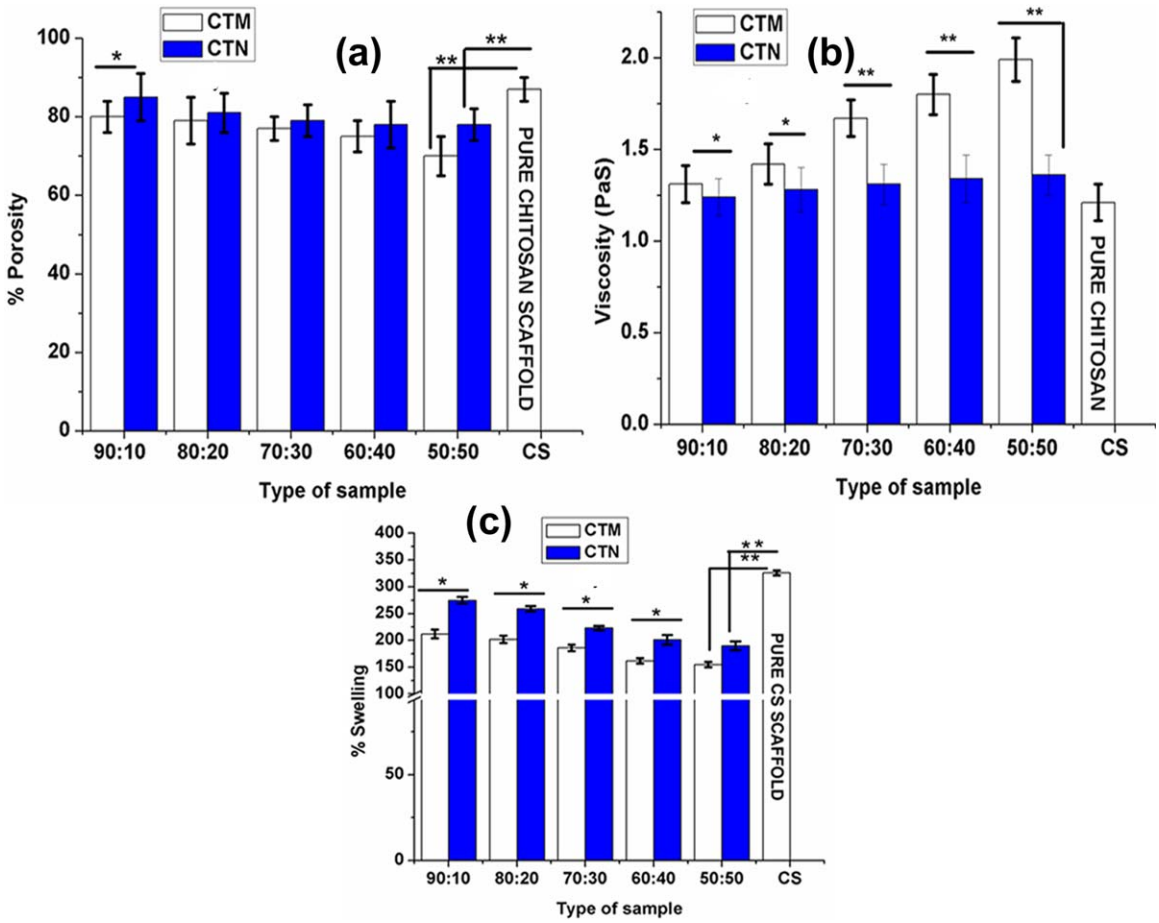

Figure 4. Porosity (a), viscosity (b), and swelling behavior (c) of CS and CS/β-TCP freeze-gelled scaffolds. [Color figure can be viewed in the online issue, which is available at wileyonlinelibrary.com.]

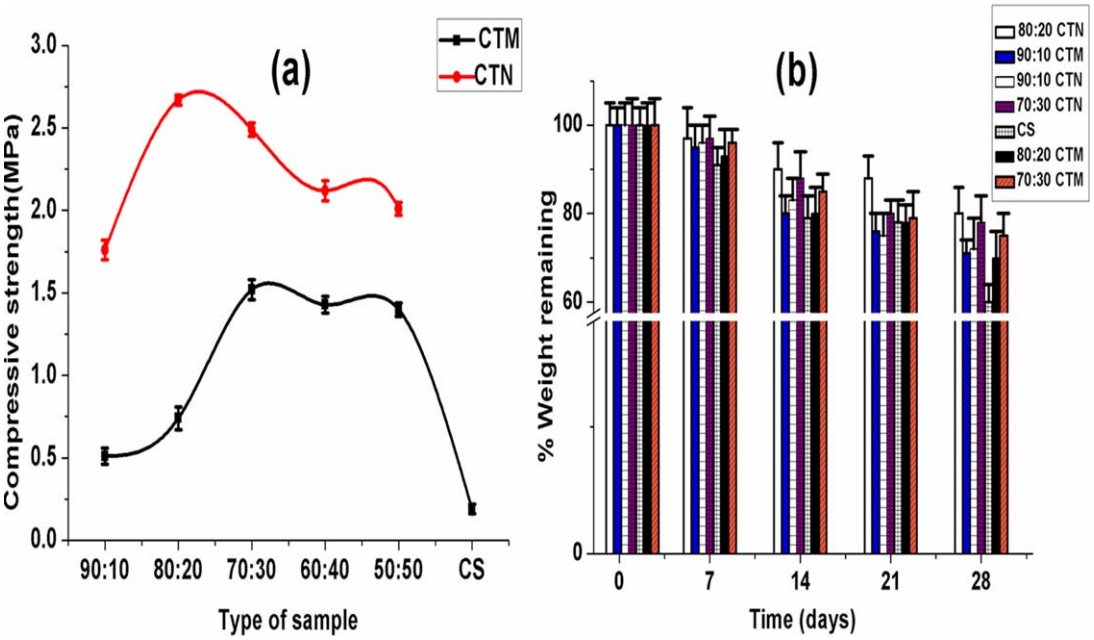

Figure 5. Compressive strength (a) and degradation pattern (b) of CS and CS/β-TCP freeze-gelled scaffolds. [Color figure can be viewed in the online issue, which is available at wileyonlinelibrary.com.]

increase in ceramic content. The decrease in swelling observed with composite scaffolds is mainly due to the incorporation of β-TCP in the polymer matrix which ultimately lead to a decrease in diffusion of water as reported earlier when wollastonite was used as filler.[17] The composite scaffolds with nano β-TCP shows an increase in swelling rate (~190–275%) than the scaffolds loaded with micro β-TCP (~155–212%) as filler. The swelling behavior of the scaffolds matches with the previously reported data.[41] Thus, the study confirms the desirable hydrophilic nature of the prepared composite scaffolds.

Mechanical Property

The scaffolds must possess enough strength to withstand the force exerted by newly formed tissue under *in vitro* stage to *in vivo* handling.[20] It has been reported that, incorporating bioceramic will enhance the mechanical strength of polymeric scaffolds.[17,39] We observed a similar trend in compressive strength of CS/β-TCP composite scaffolds. Compressive strength of CS scaffolds with micro-sized β-TCP is shown to increase with increase in β-TCP content up to 30% (CTM70 : 30) beyond which a decline in compressive strength is observed. This unusual phenomenon is due to the agglomeration of β-TCP in the polymer matrix which resulted in decreased reinforcing ability of the filler and hence compressive strength. When the particle is in nanosize, the reinforcement effect is better on a comparative scale with micro.[42] The high surface-to-volume ratio of nanosize particle and unusual chemical synergistic effects resulted in improved mechanical properties of

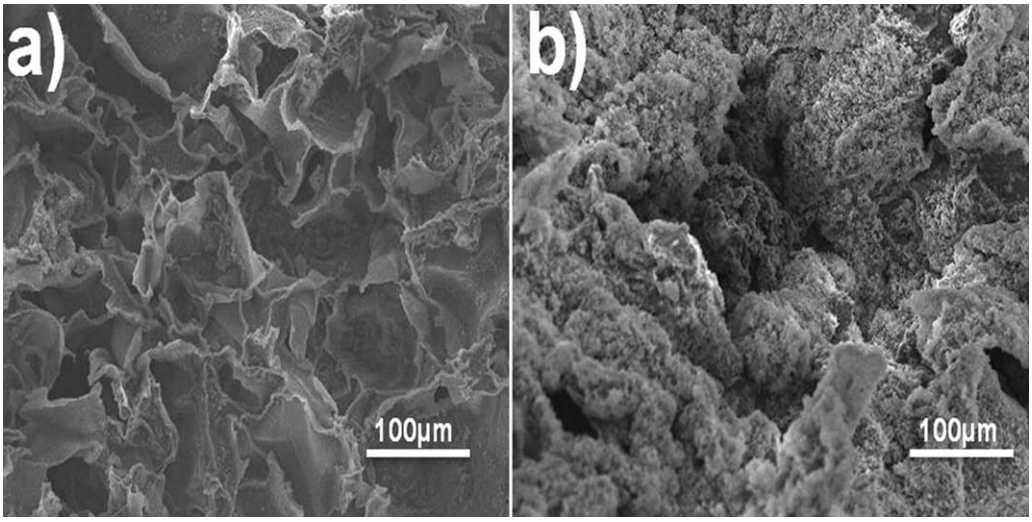

Figure 6. Apatite crystal formation on CS/β-TCP [CTM70 : 30(a) and CTN 80 : 20(b)] freeze-gelled scaffolds in SBF immersion for 3 weeks.

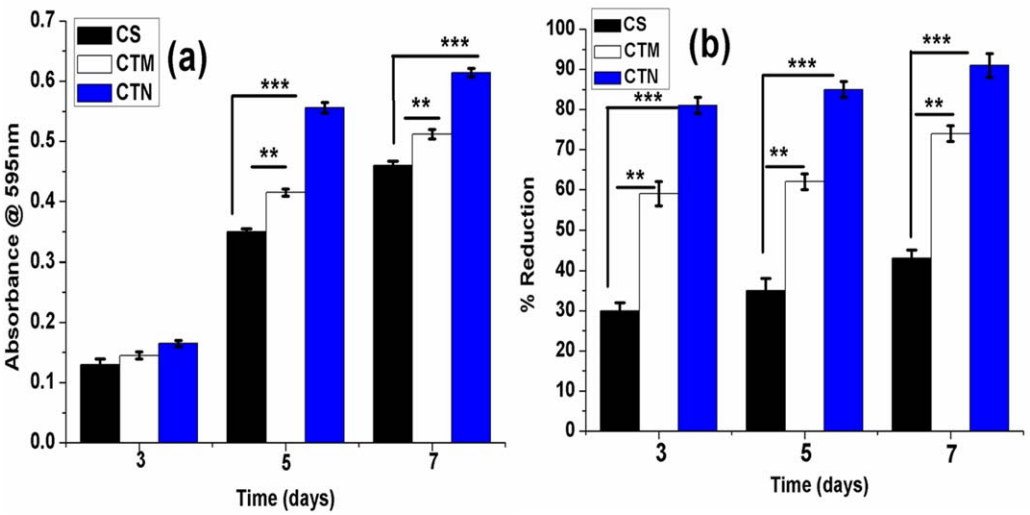

Figure 7. Metabolic activity (a) and cell proliferation (b) of hMSCs on CS and CS/β-TCP freeze-gelled scaffolds (CTM 70 : 30,CTN 80 : 20) after 3, 5, and 7 days of cell seeding. Each point represents the mean ± SD ($n = 3$). ** and *** shows significant differences between groups at $P < 0.02$ and 0.05, respectively. [Color figure can be viewed in the online issue, which is available at wileyonlinelibrary.com.]

bioceramics as reported earlier.[18] The compressive strength of the scaffolds with nano β-TCP has been increased up to 20% (CTN80 : 20) and maintained till 40% (CTN60 : 40) which meets the desired compressive strength of cancellous bone 2–10 MPa. In previous reports, the compressive strength of CS gel and 3D CS scaffold has been increased to 0.8 and 1.8 MPa, respectively, by incorporating micro β-TCP.[16,39] It is quite interesting to note that, a drastic increase in compressive strength of 2.67 MPa is achieved in our study using nanosize β-TCP. The compressive strength of all other scaffolds with varied ratios of β-TCP was shown in Table I. Figure 5(a) depicts the observed compressive strength pattern of scaffolds with varied ratios of β-TCP.

In Vitro Biodegradation Study

The rate of biodegradadation is vital to restore the entire tissue structure. So, adequate control over the rate of degradation plays a major role to be on par with the growth rate of newly formed tissue.[15] Biodegradation of the prepared CS and CS/β-TCP composite scaffolds was performed in SBF for 4 weeks. Pure CS sample found to degrade faster than (40% of its initial weight) any of the composite scaffolds prepared with varying ratios of β-TCP. The degradation pattern of the scaffolds is shown in Figure 5(b). The best result in terms of reduced degradation rate is achieved with the ratio (CTN80 : 20) as it found to degrade only ~20% of its initial weight, where as the other composite scaffolds are found to degrade as follows; CTM90 : 10 (~30%) CTM 80 : 20 (~30%), CTM70 : 30 (~25%), and CTN90 : 10 (~30%), and CTN70 : 30 (~22%). Similar trend in decreased degradation rate was also observed when hydroxy apatite was incorporated in CS matrix as reported earlier.[43] The results further reveal that addition of nano-sized β-TCP decelerates the rate of degradation than CS/micro β-TCP and pure CS scaffold.

Bioresorption Analysis

The composite scaffolds (CTM70 : 30 and CTN80 : 20) were analyzed for their *in vitro* bioactivity. Composite scaffold types

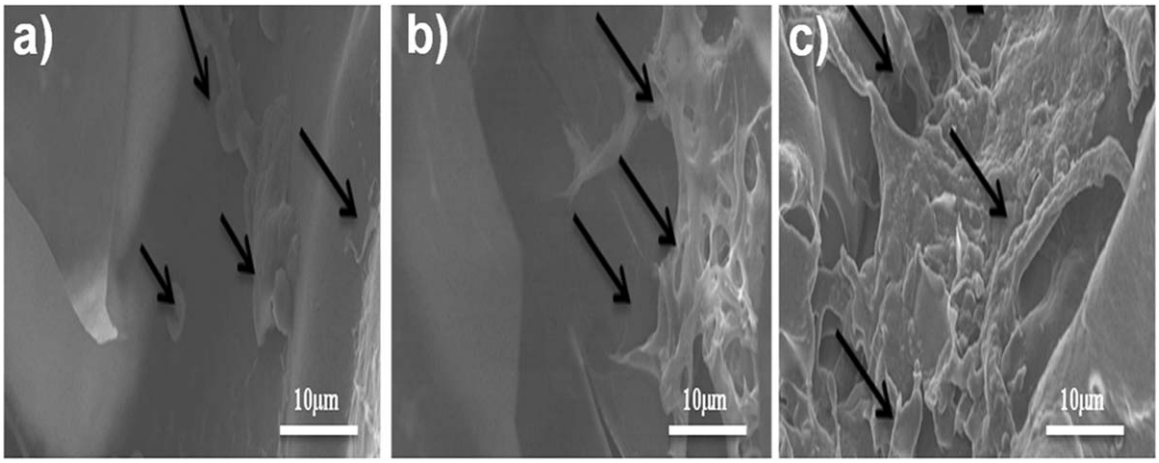

Figure 8. SEM images of cell attachment on CS/β-TCP freeze-gelled scaffold (CTN 80 : 20) surface on 3, 5, and 7 days.

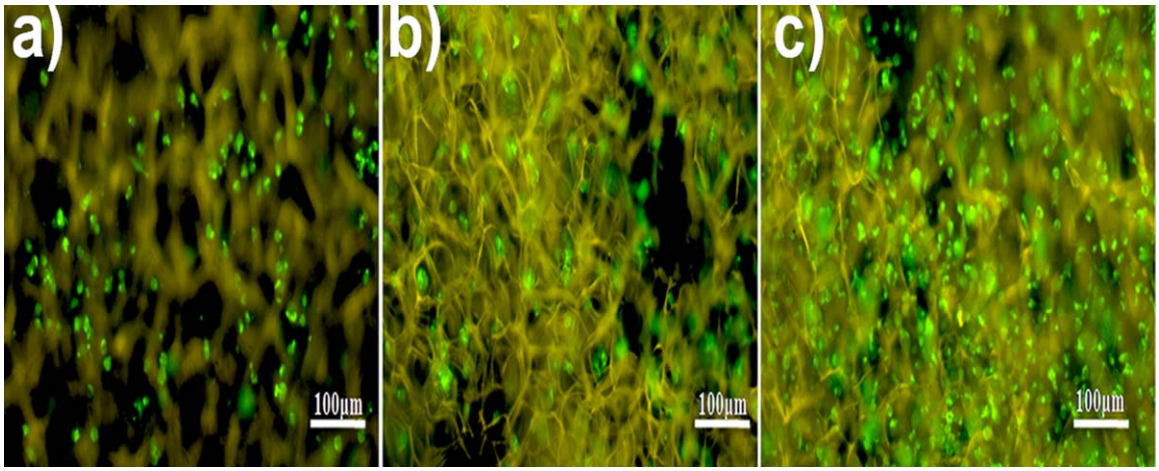

Figure 9. Florescence images of hMSCs seeded cell scaffold (CTN 80 : 20) construct after third (a), fifth (b), and seventh day. [Color figure can be viewed in the online issue, which is available at wileyonlinelibrary.com.]

CTM70 : 30 and CTN80 : 20 were selected among various scaffolds prepared based on higher mechanical strength and slower degradation rate. Formation of apatite layer on the surface of composite scaffold was found to be initiated after 7 days of soaking in SBF. Further, the amount of apatite formed was gradually increased with time and the entire surface area of the scaffold was coated with apatite after 18 days. The result is in good agreement with previous reports which suggest that covering of apatite over the entire scaffold surface takes 14–21 days.[17] Furthermore, more dense layers of apatite were formed on the surface of composite scaffolds as shown in Figure 6. The amount of apatite formed on the composite scaffold CTN80 : 20 is higher [Figure 6(b)] than that on CTM70 : 30 [Figure 6(a)]. The increase in apatite formation achieved with CS/nano β-TCP is due to uniform distribution of nano-sized bioceramic which enhanced nucleation sites in the CS polymer.[20]

Metabolic Activity and Proliferation Assay

The metabolic activity and proliferation of the scaffold types CS, CTM70 : 30, and CTN80 : 20 were evaluated by MTT and alamar blue assay, respectively. Figure 7(a,b) illustrates the experimental results. CS scaffold has shown lesser optical density (MTT value) and percentage of alamar reduction throughout the assay than CTM70 : 30 and CTN80 : 20 composite scaffolds. Incorporation of bioceramics not only improved the mechanical strength but also biocompatibility of CS scaffolds as reported earlier.[3,13]

The better cell compatibility and proliferation of composite scaffold CTN80 : 20 may be attributed to homogenous distribution of nano β-TCP in the CS matrix which in turn allows uniform nutrient permeation through the scaffold architecture.[30] The other reason for better cellular proliferation on composite scaffolds is due to the presence of Ca ions in β-TCP which triggers the proliferation of seeded cells as observed earlier with keratinocyte proliferation.[44] Results of CTM70 : 30 and CTN80 : 20 show a significant difference at $P < 0.02$, whereas CTN80 : 20 and CS scaffolds at $P < 0.05$ for both MTT and proliferation assay. Thus, this study proves that, the particle size of bioceramic has a direct effect on scaffold biocompatibility and proliferation.

Cell Attachment and Florescence Microscopy

Cell viability depends on scaffold architecture especially pore size, porosity, and interconnectivity, as reported earlier.[45] In our study, cytocompatibility of the freeze-gelled scaffolds was evaluated by culturing hMSCs up to 7 days. SEM micrographs revealed excellent cell adherence on the developed freeze-gelled scaffolds after 3, 5, and 7 days of culture as shown in Figure 8. The arrow marks in Figure 8 well depicts the attachment and spreading of cells over the scaffold surface. By Day 3, the cells found to acclimatize to scaffold environment and are found to be round in shape with slow spreading. By fifth and seventh day, spreading is profuse around the surface area of the scaffold which affirms their compatibility to the scaffold environment. The distribution and infiltration of cells on the scaffold surface and in pore walls is clearly seen with calcein staining. Third, fifth, and seventh day florescent images are shown in Figure 9(a–c), respectively. The florescent images also illustrate the proliferation and increase in cell number from Day 3 to Day 7 as reported earlier on 3D cryogels.[28] Cell attachment by SEM and florescent images confirm the biocompatibility of developed freeze-gelled scaffold.

CONCLUSIONS

CS and CS/β-TCP composite scaffolds were successfully prepared by freeze gelation method. Both pure CS and composite scaffolds have porous network with an excellent pore interconnectivity and desired porosity. The compressive strength of the CS scaffold was increased with the addition of β-TCP and maximum compressive strength of 2.67 ± 0.13 MPa is achieved with CTN80 : 20. Bioactive nature of the developed scaffolds has been confirmed by the deposition of apatite layers on their surface after 3 weeks of incubation. The cytocompatability of scaffolds was confirmed by MTT assay and proliferation by Alamar blue assay. Morphological analysis by SEM and fluorescence microscopy revealed that hMSCs were attached and well proliferated on the developed composite scaffolds. Thus, the addition

of nano β-TCP has enhanced the mechanical strength, biocompatibility, bioresorption, and decreased the degradation rates which are favorable scaffold characteristics for bone tissue regeneration. Further, CS/nano β-TCP composite scaffold is superior than composite scaffolds prepared with micro β-TCP. Hence, the developed CS-based freeze-gelled composite scaffold is proved to be a potential candidate for bone tissue engineering applications.

ACKNOWLEDGMENTS

The authors thank the Department of Biotechnology, Government of India, New Delhi for providing research facility created under the program support on tissue engineering research. The authors are also thankful to National Institute of Technology, Rourkela for providing institute fellowship to one of the authors (Siddiqui) and other necessary infrastructural facility to carry this work.

REFERENCES

1. Sabir, M. I.; Xu, X.; Li, L. *J. Mater. Sci.* **2009**, *44*, 5713.
2. Dash, M.; Chiellini, F.; Ottenbrite, R.; Chiellini, E. *Prog. Polym. Sci.* **2011**, *36*, 981.
3. Venkatesan, J.; Kim, S.-K. *Mar. Drugs* **2010**, *8*, 2252.
4. Dutta, P. K.; Dutta, J.; Tripathi, V. *J. Sci. Ind. Res.* **2004**, *63*, 20.
5. Costa-Pinto, A. R.; Reis, R. L.; Neves, N. M. *Tissue Eng. Part B Rev.* **2011**, *17*, 331.
6. Li, Z.; Ramay, H. R.; Hauch, K. D.; Xiao, D.; Zhang, M. *Biomaterials* **2005**, *26*, 3919.
7. Salgado, A. J.; Coutinho, O. P.; Reis, R. L. *Macromol. Biosci.* **2004**, *4*, 743.
8. Caoand, H.; Kuboyama, N. *Bone* **2010**, *46*, 386.
9. Nairand, L. S.; Laurencin, C. T. *Prog. Polym. Sci.* **2007**, *32*, 762.
10. Chuenjitkuntaworn, B.; Inrung, W.; Damrongsri, D.; Mekaapiruk, K.; Supaphol, P.; Pavasant, P. *J. Biomed. Mater. Res. A* **2010**, *94*, 241.
11. Uchida, M.; Agata, H.; Sagara, H.; Shinohara, Y.; Kagami, H.; Asahina, I. *J. Biomed. Mater. Res. A* **2009**, *91*, 84.
12. Wongwitwichot, P.; Kaewsrichan, J.; Chua, K.; Ruszymah, B. *Open Biomed. Eng. J.* **2010**, *4*, 279.
13. Janaki, K.; Elamathi, S.; Sangeetha, D. *Artif. Organs (India)* **2009**, *20080701*, 21.
14. Hsieh, C.-Y.; Tsai, S.-P.; Ho, M.-H.; Wang, D.-M.; Liu, C.-E.; Hsieh, C.-H.; Tseng, H.-C.; Hsieh, H.-J. *Carbohydr. Polym.* **2007**, *67*, 124.
15. Yuan, N.-Y.; Lin, Y.-A.; Ho, M.-H.; Wang, D.-M.; Lai, J.-Y.; Hsieh, H.-*J. Carbohydr. Polym.* **2009**, *78*, 349.
16. Ruiran, H.; Aihua, Y.; Deping, W.; Wen-hai, H. *J. Funct. Mater.* **2010**, *41*, 148.
17. Zhao, L.; Chang, J. *J. Mater. Sci. Mater. Med.* **2004**, *15*, 625.
18. Jiang, L.; Li, Y.; Wang, X.; Zhang, L.; Wen, J.; Gong, M. *Carbohydr. Polym.* **2008**, *74*, 680.
19. Bhardwaj, N.; Chakraborty, S.; Kundu, S. C. *Int. J. Biol. Macromol.* **2011**, *49*, 260.
20. Causa, F.; Netti, P.; Ambrosio, L.; Ciapetti, G.; Baldini, N.; Pagani, S.; Martini, D.; Giunti, A. *J. Biomed. Mater. Res. A* **2006**, *76*, 151.
21. Bhattacharya, C.; Kumar, N.; Sagiri, S. S.; Pal, K.; Ray, S. S. *J. Pharm. Bioallied Sci.* **2012**, *4*, 155.
22. Jiang, T.; Abdel-Fattah, W. I.; Laurencin, C. T. *Biomaterials* **2006**, *27*, 4894.
23. Pati, F.; Kalita, H.; Adhikari, B.; Dhara, S. *J. Biomed. Mater. Res. A* **2013**, *101*, 2526.
24. Bi, L.; Cao, Z.; Hu, Y.; Song, Y.; Yu, L.; Yang, B.; Mu, J.; Huang, Z.; Han, Y. *J. Mater. Sci. Mater. Med.* **2011**, *22*, 51.
25. Kokubo, T.; Kushitani, H.; Sakka, S.; Kitsugi, T.; Yamamuro, T. *J. Biomed. Mater. Res.* **1990**, *24*, 721.
26. Bissoyiand, A.; Pramanik, K. *Cryoletters* **2013**, *34*, 453.
27. Xu, W.; Ma, J.; Jabbari, E. *Acta Biomater.* **2010**, *6*, 1992.
28. Singh, D.; Nayak, V.; Kumar, A. *Int. J. Biol. Sci.* **2010**, *6*, 371.
29. Xiong, Y.; Zeng, Y.-S.; Zeng, C.-G.; Du, B.-I.; He, L.-M.; Quan, D.-P.; Zhang, W.; Wang, J.-M.; Wu, J.-L.; Li, Y.; Li, J. *Biomaterials* **2009**, *30*, 3711.
30. Karande, T. S.; Ong, J. L.; Agrawal, C. M. *Ann. Biomed. Eng.* **2004**, *32*, 1728.
31. Yang, S.; Leong, K.-F.; Du, Z.; Chua, C.-K. *Tissue Eng.* **2001**, *7*, 679.
32. Whang, K.; Healy, K.; Elenz, D.; Nam, E.; Tsai, D.; Thomas, C.; Nuber, G.; Glorieux, F.; Travers, R.; Sprague, S. *Tissue Eng.* **1999**, *5*, 35.
33. She, Z.; Zhang, B.; Jin, C.; Feng, Q.; Xu, Y. *Polym. Degrad. Stab.* **2008**, *93*, 1316.
34. Spataru, M.; Tardei, C.; Nemtanu, M. R.; Bogdan, F. *Revue Roumaine de Chimie* **2008**, *53*, 955.
35. Thein-Han, W.; Misra, R. *Acta Biomater.* **2009**, *5*, 1182.
36. Rai, B.; Oest, M. E.; Dupont, K. M.; Ho, K. H.; Teoh, S. H.; Guldberg, R. E. *J. Biomed. Mater. Res. A* **2007**, *81*, 888.
37. Potschke, P.; Fornes, T.; Paul, D. *Polymer* **2002**, *43*, 3247.
38. Kamal, M.; Mutel, A. *J. Polym. Eng.* **1985**, *5*, 293.
39. Yin, Y.; Ye, F.; Cui, J.; Zhang, F.; Liand, X.; Yao, K. *J. Biomed. Mater. Res. A* **2003**, *67*, 844.
40. Yilgor, P.; Sousa, R. A.; Reis, R. L.; Hasirciand, N.; Hasirci, V. *J. Mater. Sci. Mater. Med.* **2010**, *21*, 2999.
41. Nandagiri, V. K.; Gentile, P.; Chiono, V.; Tonda-Turo, C.; Matsiko, A.; Ramtoola, Z.; Montevecchi, F. M.; Ciardelli, G. *J. Mech. Behav. Biomed. Mater.* **2011**, *4*, 1318.
42. Zhang, L.; Webster, T. *J. Nano Today* **2009**, *4*, 66.
43. Maachou, H.; Bal, K.; Bal, Y.; Chagnes, A.; Cote, G.; Alliouche, D. *Trends Biomater. Artif. Organs* **2008**, *22*, 15.
44. Boyce, S. T.; Ham, R. G. *J. Invest. Dermatol.* **1983**, *81*, 33.
45. Sechriest, V. F.; Miao, Y. J.; Niyibizi, C.; Westerhausen-Larson, A.; Matthew, H. W.; Evans, C. H.; Fu, F. H.; Suh, J. K. *J. Biomed. Mater. Res.* **2000**, *49*, 534.